The Astrophysical Journal, 592:176–187, 2003 July 20

NEUTRAL HYDROGEN ASSOCIATED WITH NGC 7129

H. E. Matthews[1]
Herzberg Institute of Astrophysics, National Research Council of Canada, 5071 West Saanich Road, Victoria, BC V9E 2E7, Canada; hem@jach.hawaii.edu

C. R. Purton, R. S. Roger, and P. E. Dewdney
Dominion Radio Astrophysical Observatory, Herzberg Institute of Astrophysics, National Research Council of Canada, P.O. Box 248, Penticton, BC V2A 6J9, Canada

and

G. F. Mitchell
Department of Astronomy and Physics, Saint Mary's University, Halifax, NS B3H 3C3, Canada
Received 2002 January 28; accepted 2003 April 2

ABSTRACT

Observations of the environment of the star-forming region NGC 7129 obtained with an angular resolution of 1′ in the 21 cm line of H I are described. Two features of the image are extensively discussed: (1) a ring of H I emission about 30′ in extent and (2) a relatively dense concentration of H I with unusually wide line profiles positionally coincident with the B star BD +65°1638. The H I ring is consistent with photodissociation of H_2 by the interstellar UV radiation field at the surface of an extended molecular cloud in which both BD +65°1638 and NGC 7129 are situated. We further show that BD +65°1638 appears to be an unusual example of a "dissociating star" surrounded by an extensive region of photodissociated H_2 and accompanied by a small H II region. The derived spectral type (B2.5) and the absolute magnitude for BD +65°1638 further suggest that the latter is very close to the birthline. The very young stellar age implied by the parameters of the H I region, considerably less than 10^4 yr, is discussed, and the properties of the H I region are compared with those of the prototype for this rare class of objects. We discuss both aspects within the context of star formation in NGC 7129.

Subject headings: ISM: atoms — ISM: clouds — ISM: individual (NGC 7129) — reflection nebulae — stars: formation — stars: pre–main-sequence

1. INTRODUCTION

NGC 7129 is a reflection nebula in a star-forming region at a distance of about 1 kpc (Racine 1968), which has been studied extensively at optical, infrared, radio, and millimeter to submillimeter wavelengths. Within the nebula there are two B stars, BD +65°1637 and BD +65°1638, both contained within an apparent cavity in the CO emission associated with NGC 7129 (Bechis et al. 1978). The unusual Ae/Be star LkHα 234 is situated within bright CO emission at the eastern edge of NGC 7129. An overview of the region is presented in Figure 1; with 1′ resolution, observations of CO show ambient gas with typical local standard of rest (LSR) velocities between −13 and −9 km s^{-1} and a complex low-velocity outflow structure extending in projection over about 12′, in which the gas is mostly blueshifted by about 5 km s^{-1} in the southwest and predominantly redshifted by the same amount in the northeast (Edwards & Snell 1983). Including LkHα 234 there are at least three apparent centers of star-forming activity in NGC 7129; IRS 1 (Liseau & Sandell 1983), 4.′5 to the north of LkHα 234, shows high-velocity wings in the CO emission profile, while a far-infrared source 3′ to the south (FIRS 2; see also Eiroa, Palacios, & Casali 1998) coincides with a molecular concentration in CO (Edwards & Snell 1983; Hartigan & Lada 1985) and NH_3 (Güsten & Marcaide 1986) and a molecular outflow (Miskolczi et al. 2001).

With better angular resolution molecular line observations reveal that the cavity is at least partially bounded by dense ridges of material to the east, south, and west (Mitchell & Matthews 1994; Miskolczi et al. 2001), as shown schematically in Figure 1. LkHα 234 in particular, embedded within dense molecular gas at the eastern edge of the cavity, is a member of a recently identified cluster of stars (Fuente et al. 2001), one of which is the source of an optical jet that projects well into the cavity (Ray et al. 1990). LkHα 234 and the other cluster members may have been formed in response to compression of the molecular gas at the edge of the cavity, which Mitchell & Matthews (1994) suggest may have been produced by a stellar wind from one of the B stars in the cavity. A second dense clump of gas just to the north of LkHα 234 suggests star formation remains ongoing within this region.

In this paper we investigate the structure and dynamics of the NGC 7129 region on a larger scale via the first detailed study of neutral hydrogen (H I, at a wavelength of 21 cm), obtained with an angular resolution of about 1′ (equivalent to 0.29 pc at a distance of 1 kpc).

2. OBSERVATIONS AND DATA PROCESSING

The observations were carried out using the Dominion Radio Astrophysical Observatory (DRAO) Synthesis Telescope (Landecker et al. 2000) during September 1995. The field was centered at (R.A. = $21^h43^m06^s.2$, decl. = 66°06′56″ [J2000.0]), close to LkHα 234. The Galactic coordinates of NGC 7129 ($l = 104.°7$, $b = 9.°1$) place it outside the original latitude limit of the Canadian Galactic Plane

[1] Also at Joint Astronomy Centre, 660 North A'ohōkū Place, Hilo, HI 96720-6030. Present address: Dominion Radio Astrophysical Observatory, Hertzberg Institute of Astrophysics, National Research Council of Canada, P.O. Box 248, Penticton, BC V2A 6J9, Canada.

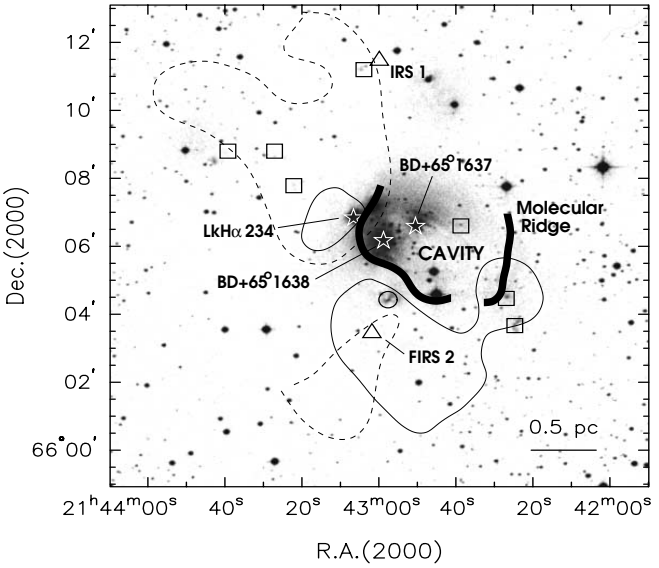

FIG. 1.—Overview of the NGC 7129 region superposed on an image taken from the Digitized Sky Survey (DSS) (red filter), showing the three bright young stars LkHα 234, BD +65°1637, and BD +65°1638 within the nebulosity (*star symbols*). We also show some of the many Herbig-Haro objects (*squares*), indicative of star formation within NGC 7129, the positions of two bright infrared and far-infrared sources (IRS 1 and FIRS 2; *triangles*) coincident with the secondary star-forming center, and the location of a reflection nebula (RNO 138; *circle*). The outlined regions show the extent of CO 1–0 low-velocity outflow emission as mapped by Edwards & Snell (1983); the continuous and dashed contours, respectively, indicate blueshifted and redshifted material. Observations with higher angular resolution of CO 2–1 and CO 3–2 transitions reveal dense molecular ridges (*thick lines*), which appear at ambient velocities and surround a pronounced cavity (as indicated) in the molecular gas distribution. CO has not been mapped with good resolution in the northwest sector.

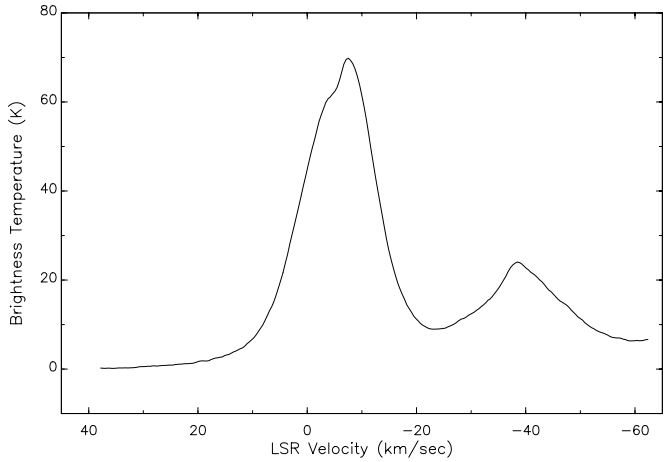

FIG. 2.—Mean H I emission velocity profile for the NGC 7129 field, averaged over a 1° radius about the field center. H I emission shown in subsequent figures is relative to this reference level.

Survey (CGPS; English et al. 1998; Taylor et al. 2003), and these observations were not part of the latter. NGC 7129 was, however, observed in precisely the standard manner (Landecker et al. 2000) as for all CGPS fields. We briefly describe the procedure below.

In these observations the *uv*-plane was fully sampled over 12^h in hour angle and over all interferometer spacings from 12.9 to 617.1 m. A total spectrometer bandwidth of 0.5 MHz was employed for the spectral line observations, centered at the frequency of the H I line (1420.406 MHz) and offset to an LSR velocity[2] of -10 km s^{-1}. The channel spacing was 0.412 km s^{-1} and the spectral resolution 0.66 km s^{-1}. The spectral line data were obtained from the average of both right- and left-hand circularly polarized observations.

Continuum data were obtained concurrently with H I synthesis data from two bands 15 MHz wide symmetrically placed about the H I line. These data were compared with those from the present H I synthesis data set within the velocity range 8.6–41.5 km s^{-1} and identified as having negligible H I emission at the rms noise level of about 0.6 K brightness temperature. The flux densities of the five brightest pointlike continuum sources in these maps were then used to obtain correct scaling of the H I line synthesis data set, and the continuum synthesis data set was then subtracted from the synthesis spectral line data cube, resulting in pure H I line data.

[2] All velocities in this paper are given with respect to the local standard of rest (LSR).

Short-spacing H I data were obtained using the DRAO 26 m telescope in the prescribed manner for observations for this purpose, on a square grid of 256 spectra with a spacing of 16′ in equatorial coordinates. The short-spacing and synthesis data cubes were then combined in the standard way (Higgs 1999) to provide a final data cube containing all spatial frequencies from 0 to 617 m inclusive. The resultant high-quality data thus has complete interferometer visibility (*uv*) coverage within the physical limits of the telescope. The final synthesized beam has half-power widths of 64″.0 and 59″.7 at a major-axis position angle of about $-75°$. The rms noise in the individual H I line channel maps is about 4.4 K in brightness temperature (T_b; equivalent to 23 mJy beam^{-1}), and for the continuum data the rms noise is 0.28 mJy beam^{-1}.

From this final data set a mean H I profile was determined from the central 1° radius and subtracted from the complete data cube to facilitate our study of small-scale structures in the field. The average spectrum of this subtracted material is shown in Figure 2; the two main peaks at about -8 and -39 km s^{-1} correspond to the LSR velocities of the Orion and Perseus arms of the Galaxy, respectively. It is clear that at the velocity range of principal interest here (-10 to -15 km s^{-1}) the slope of the mean H I profile is steep, and small changes in the local shape of this profile will result in significant residual emission in the mean H I–subtracted map data. We discuss this further as necessary below.

3. OBSERVATIONAL RESULTS

In any observation of neutral hydrogen with a line of sight passing through the Galactic plane there will be a variety of apparently coherent structures detected in the subtracted data. In particular, as is common in such observations, in the NGC 7129 field we find a considerable number of ribbon-like features at specific velocities having typical velocity ranges of 1–2 km s^{-1}, length-to-width ratios of 10 or more, and peak H I line strengths of up to about 20 K. These are the dominant structural component of the interstellar medium as viewed in H I at spatial scales of 1′–30′ (Ghazzali, Joncas, & Jean 1999; Gibson et al. 2000). However, most of these within the present field cannot be

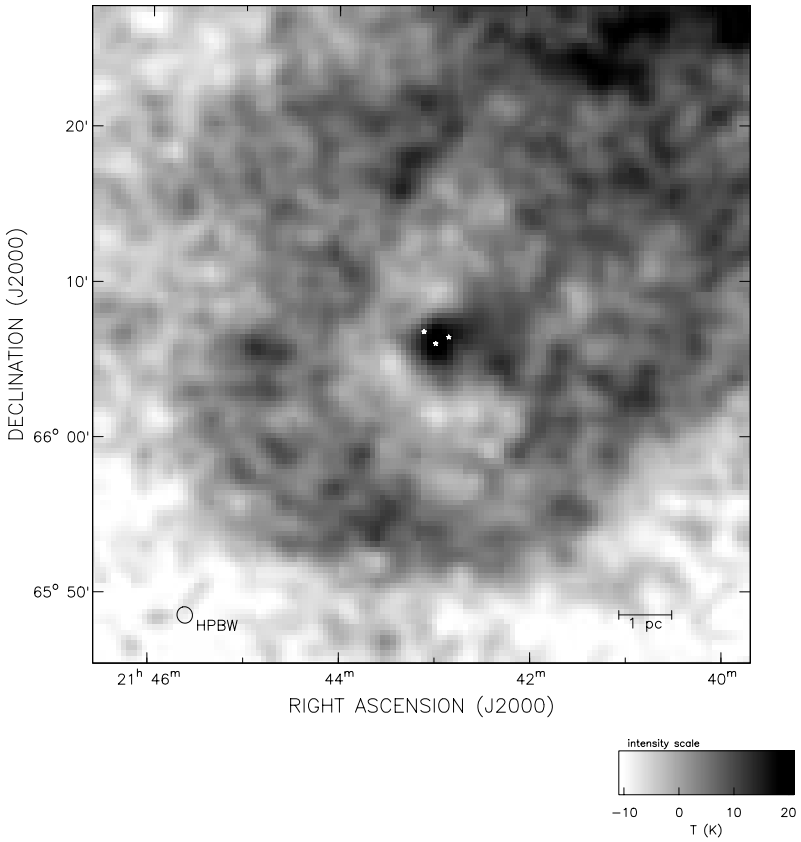

FIG. 3.—H I emission averaged over the LSR velocity range −10.2 to −13.1 km s^{-1}, showing the H I "ring" and "knot" features. The size of the synthesized beam is shown by the circle marked "HPBW," and the linear scale is indicated at lower right for the distance of 1 kpc. The rms noise in this map is $T_b = 2.1$ K. The steep gradient in residual H I emission after subtraction of the mean H I background (see Fig. 2) is evident in this representation. Positions of the three stars referred to in the text, from left to right, LkHα 234, BD +65°1638, and BD +65°1637 are indicated at the image center. BD +65°1638 coincides most closely with the center of the H I knot.

clearly associated with NGC 7129 itself since (1) they are at LSR velocities quite different from the associated molecular cloud and (2) with one possible exception (see § 3.3) they do not possess spatial structure that suggests any such association.

In this paper we confine our attention mostly to two unusual H I emission features for which there is the strong suggestion of a physical link with NGC 7129. We have found (1) a ring of H I surrounding NGC 7129, at the center of which is (2) a compact H I feature having a broad-line profile. Both features have LSR velocities of about −12 km s^{-1}, well within the range of velocities of the molecular material associated with NGC 7129. We will use the terms "ring" and "knot" in simple reference to these components of the H I emission. In Figure 3 we show an image of the H I emission integrated over a velocity range typical of that for NGC 7129, covering approximately the central half-degree of the observed field, which displays these features very clearly.

3.1. H I *Ring*

The apparent ring of H I emission has an approximate outer diameter of about 30′ (equivalent to 8.7 pc at the distance of 1 kpc), and an inner diameter of about 18′. It has a visible coherent structure extending over about 4.5 km s^{-1} in velocity, centered on $V(\mathrm{LSR}) = -12.0$ km s^{-1}. In projection it surrounds the nebulosity and molecular material associated with NGC 7129 and merges with extensive bright residual H I emission toward the northwest. The center of the ring, estimated by trial-fitting circles of different sizes, is at R.A. = $21^h42^m59\overset{s}{.}6 \pm 3\overset{s}{.}3$, decl. = 66°06′56″ ± 40″ (J2000.0), within the central group of bright stars BD +65°1638, BD +65°1637, and LkHα 234.

In Figure 4 we show a series of H I images from consecutive velocity channels to illustrate the changing structure of the ring with radial velocity. The apparent structure progresses from a thick shell with a small central cavity, at the most redshifted velocities (−10.0 km s^{-1}), to a thin shell with a large central cavity and roughly the same outer diameter, at the most blueshifted velocities. The ringlike structure is most clearly seen in the southeast quadrant. However, we have found no obvious "cap" (which might be taken to be the signature of an expanding shell) at either of the velocity extremes. We made an attempt to discern such caps by obtaining cross sections across the diameter of the ring for adjacent velocity ranges. These were found to be remarkably flat and indicate that any expansion or contraction present must have velocities less than 1.0 km s^{-1} with respect to the mean velocity.

3.2. H I *Knot*

The bright, compact H I knot almost at the center of the field is one of the most striking and intriguing aspects of the NGC 7129 H I data. The peak intensity of this feature

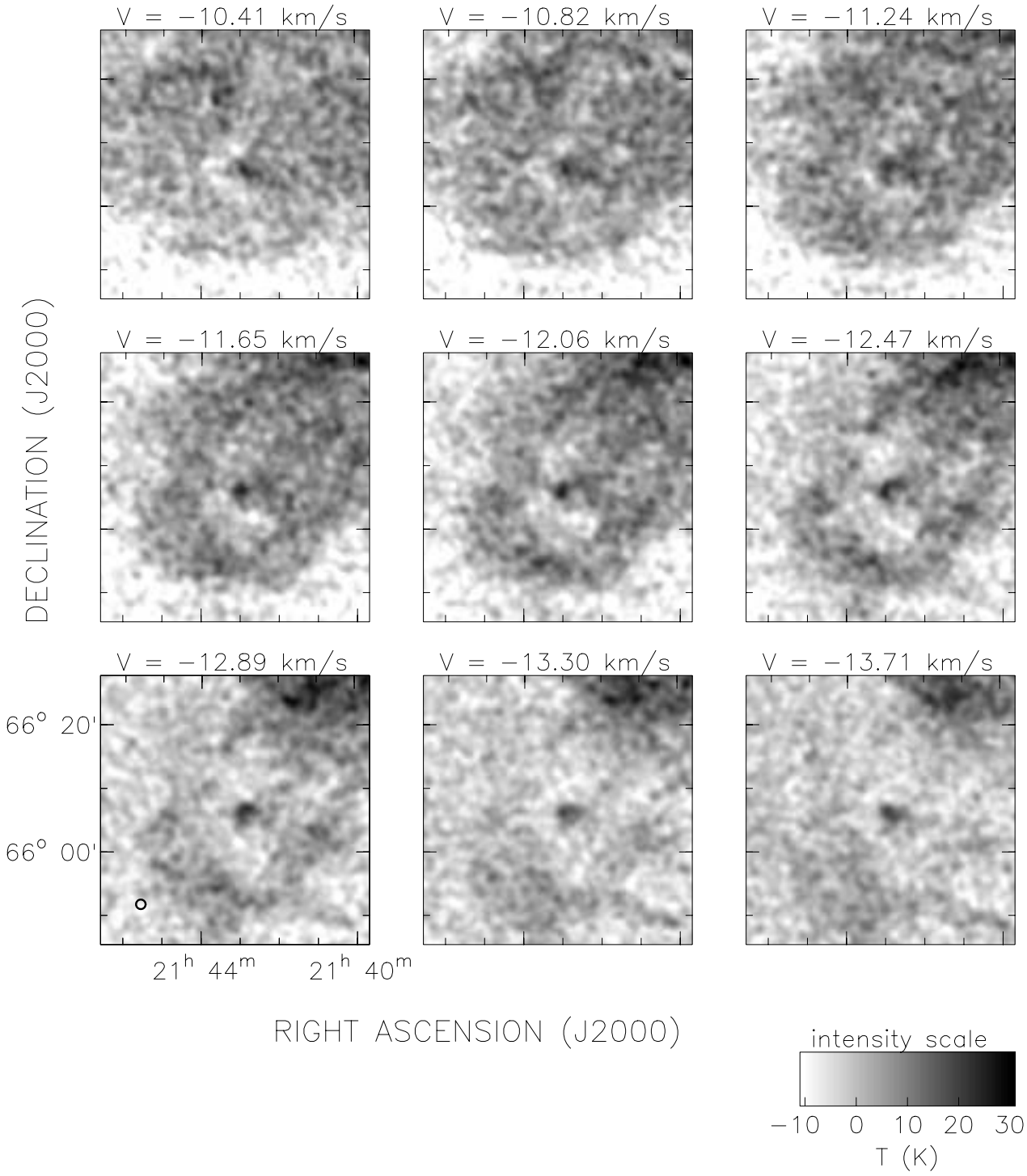

FIG. 4.—H I emission over a sequence of neighboring velocity channels near the center of the NGC 7129 field, illustrating how the structure of the H I ring changes with velocity. The central LSR velocity is indicated at the top of each frame. The channel separation is 0.412 km s^{-1}, and the velocity resolution is 0.66 km s^{-1}. The H I data were convolved to an effective beam size of 1.′5, as shown by the circle at lower left.

coincides within the measurement errors (15″) with the position of the B3 star BD +65°1638, the measured offset from the latter being 8″. The H I knot is well resolved and somewhat elongated, with angular diameters after deconvolution from the 1′ synthesized beam of 4.′5 × 2.′9, corresponding to physical dimensions of 1.3 × 0.84 pc at the distance of NGC 7129. The two other nearby stars, LkHα 234 and BD +65°1637, are offset from the center of the H I knot by 62″ and 56″, respectively, but are well within its total projected extent. The relative positions of the stars, the H I knot, and other compact sources are shown in Figure 5, and the positions of these objects collected together in Table 1. Figure 5 shows also that BD +65°1638 is embedded in a marked reflection nebula, as noted by Hartigan & Lada (1985).

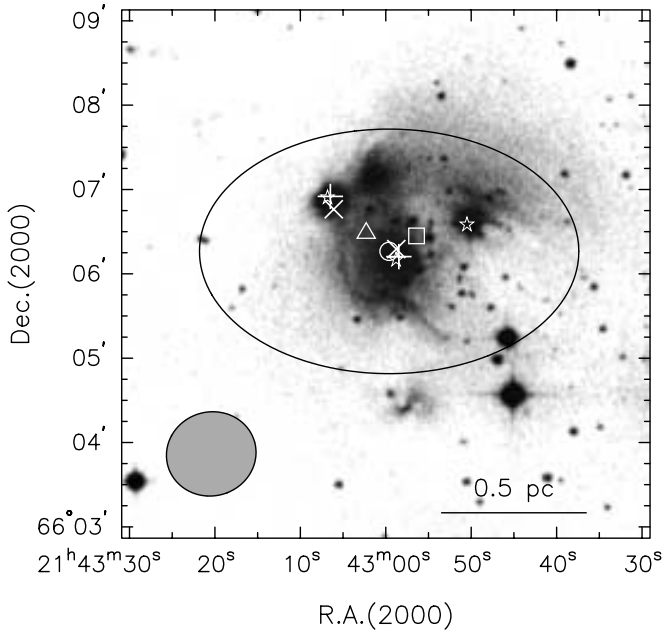

FIG. 5.—Image of NGC 7129 taken from the DSS (red filter), centered on BD +65°1638. The bright stars (from left to right) LkHα 234, BD +65°1638, and BD +65°1637 are marked by star symbols. Symbols indicate objects discussed in the text. The positions of these and other objects are listed in Table 1. The extent of the H I knot (estimated center marked by the circle), deconvolved from the beam size, is indicated by the large ellipse. Other symbols mark 1420 MHz radio continuum sources (*crosses*) from the present data, the centimeter-wave radio positions measured by Skinner et al. (1993) for BD +65°1638 and LkHα 234 (*plus signs*) by using the VLA, and the infrared objects IRAS 21418+6552 (*triangle*) and IRAS X2141+658 (*square*). The synthesized beam to half-power is shown at lower left, and a scale bar for 0.5 pc, at the distance of NGC 7129 of 1 kpc, is given at lower right.

3.2.1. *Velocity Structure*

Figure 6 (*top*) shows the H I spectrum from the central pixel of the knot. The line emission is both unusually broad (about 9 km s^{-1} FWHM) and quite strong ($T_b = 25$ K) when compared with the typical H I emission remaining in the NGC 7129 region after subtraction of the large-scale line emission components. The unusual nature of the H I knot is especially clear when displayed as a position-velocity diagram in Figure 6 (*bottom*). If the larger velocity width were attributed to thermal motion, it would indicate a kinetic temperature of about 1800 K; although some gas at this temperature and higher may be expected, bulk motion seems a more likely explanation (see § 7). Finally in passing we note that at -11.9 km s^{-1} the peak velocity of the H I knot is rather more negative than that of ambient molecular gas in the vicinity.

3.2.2. H I *Density Estimates*

The peak H I column density of the knot is estimated as 2.6×10^{20} cm^{-2}. Adopting a highly simplified model of the H I distribution, in this case a homogeneous sphere of mean diameter 1.07 pc, suggests a mean hydrogen gas density of 81 cm^{-3}. Alternatively, the average column density over the knot is 1.6×10^{20} cm^{-2}, and combining this with the solid angle and assumed distance gives a total H I mass of 1.2 $M_\odot$. Assuming spherical geometry, the latter result implies a mean gas density of 89 cm^{-3}. Hence, although the H I radial profile indicates some central concentration of the gas distribution, the fact that similar values for the average gas density can be derived for the simple model from different measurements suggests that a homogeneous sphere is indeed a reasonable model for the purposes of obtaining the gross parameters of the H I knot.

3.2.3. *Associated Continuum Emission*

Using the 1420 MHz continuum image obtained concurrently with the spectral line data, we searched for radio continuum emission in the region of the knot. Figure 7 shows the central portion of this image; a radio continuum source coincident with BD +65°1638 is seen, which shows a significant extension to the northeast overlapping the position of LkHα 234. Treating the continuum emission as a pair of unresolved sources we derive flux densities of 2.2 ± 0.3 and 0.9 ± 0.3 mJy, respectively. The continuum source positions determined (see Table 1 and Figs. 5 and 7) are coincident

TABLE 1
POSITIONS WITHIN THE NGC 7129 REGION

	R.A. (J2000.0)	Decl. (J2000.0)	Offset[a] (arcsec)	Notes
BD +65°1638	21 42 58.8	66 06 10	...	Catalog position
21 cm continuum	21 42 58.8 ± 0.7	66 06 18 ± 4	8	This paper
Centimeter-wave continuum	21 42 58.48	66 06 12.3	3	Skinner et al. 1993
H I knot (peak)	21 42 59.6 ± 2.3	66 06 16 ± 15	8	This paper
IRAS X2141+658	21 42 56.4	66 06 27	22	*IRAS* SSS[b]
IRAS 21418+6552	21 43 02.3 ± 1.0	66 06 29 ± 10	29	*IRAS* PSC[c]
H I ring center	21 42 59.6 ± 3.3	66 06 56 ± 40	46	This paper
BD +65°1637	21 42 50.5	66 06 35	56	Catalog position
LkHα 234	21 43 06.82	66 06 54.3	62	Clements & Argyle 1984
21 cm continuum (LkHα 234)	21 43 06.1 ± 1.5	66 06 46 ± 13	9[d]	This paper
Centimeter-wave continuum (LkHα 234)	21 43 06.48	66 06 55.1	2[d]	Skinner et al. 1993

NOTE.—Units of right ascension are hours, minutes, and seconds, and units of declination are degrees, arcminutes, and arcseconds.

[a] With respect to BD +65°1638, except as noted.
[b] *IRAS* Small Scale Structure Catalogue 1988.
[c] *IRAS* Point Source Catalogue 1988.
[d] With respect to LkHα 234.

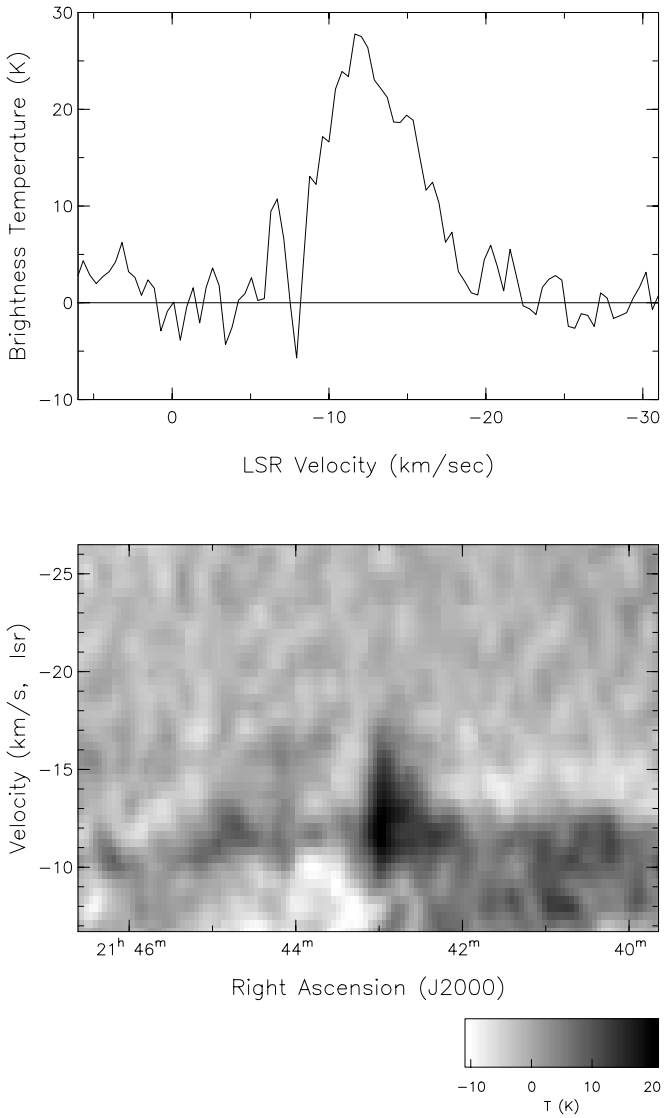

FIG. 6.—Unusual velocity characteristic of the H I knot at the center of NGC 7129. *Top*: Velocity profile at the central pixel. The width to half-power of about 9 km s^{-1} is considerably in excess of that of H I line emission in this region. *Bottom*: Right ascension–velocity slice of the H I data cube, averaged over the declination range of 80″ centered on 66°06′46″, through the center of the H I knot. The large velocity width of the central bright knot is clearly evident in this image and distinct from the general H I emission.

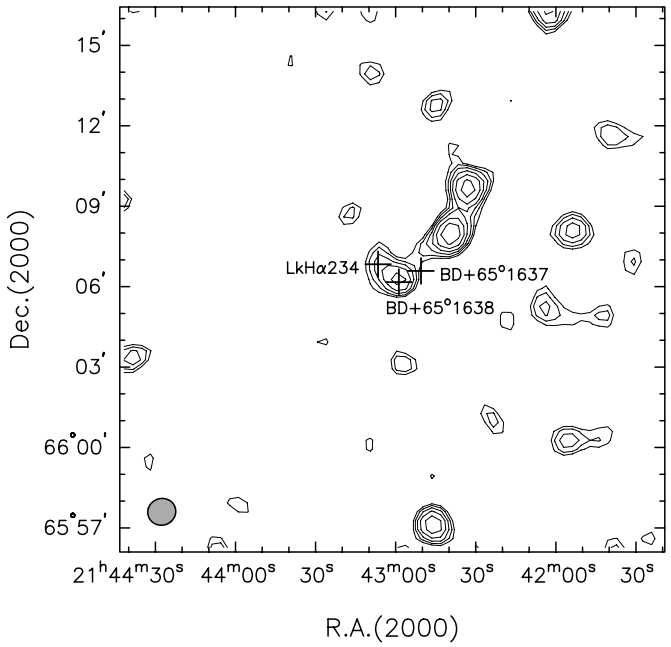

FIG. 7.—Radio continuum emission at 1420 MHz. Positions of stellar objects central to NGC 7129 are identified. BD +65°1638 is coincident with a 2.2 mJy radio source, and the extension of the contours of the latter to the northeast indicate a flux density for LkHα 234 of about 0.9 mJy. All other sources in this image are most likely extragalactic in nature. The contour levels are 0.5, 0.7, 1.0, ... mJy $beam^{-1}$, increasing by factors of $\sqrt{2}$. The size of the synthesized beam to half-power is indicated at lower left.

within the errors with BD +65°1638 and LkHα 234, respectively.

There are several other published radio continuum observations of the NGC 7129 region. In particular Skinner, Brown, & Stewart (1993) detected BD +65°1638 serendipitously in an extensive survey of Herbig Ae/Be stars, including LkHα 234, using the VLA at wavelengths of 3.6 and 6 cm. After correcting their observations for primary beam attenuation we derive integrated flux densities of 2.0 ± 0.2 and 2.2 ± 0.2 mJy at wavelengths 3.6 and 6 cm, respectively. Taking these results together with our 21 cm datum shows that BD +65°1638 has a flat centimeter-wave spectrum, consistent with an optically thin H II region around the star. The source is partially resolved at 3.6 cm with the smaller $20\farcs2 \times 9\farcs6$ synthesized beamwidth, consistent also with our estimate (see § 5.1) that the H II region is about 37″ in diameter.

Other reported radio continuum observations of BD +65°1638 are less conclusive. In three cases (Avila, Rodríguez, & Curiel 2001; Snell & Bally 1986; White & Gee 1986) the small synthesized beam would have greatly overresolved the ionized region around BD +65°1638. In addition the 1.4 GHz NRAO VLA Sky Survey (NVSS) archive (Condon et al. 1998) covers this region but does not show a catalog entry for a continuum source at the position of the H I knot. Our measured flux density is significantly below the formal limiting flux density of the NVSS (2.9 mJy $beam^{-1}$).

LkHα 234 also has been reported previously as a radio source (Avila et al. 2001; Tofani et al. 1995; Skinner et al. 1993 and references therein). However, Cabrit et al. (1997) established that the radio source is in fact associated with a 10 μm embedded source, IRS 6, 2″.3 northwest of LkHα 234, rather than with LkHα 234 itself. Our present measurement at 1420 MHz extends the centimeter-wave continuum spectrum of this object to longer wavelengths by a factor of 3 and confirms the spectral index of 0.6 characteristic of an ionized wind, as reported by Skinner et al. (1993).

3.2.4. *Infrared Emission*

The *IRAS* Point Source Catalogue (1988; PSC) shows an infrared point source, IRAS 21418+6552, coincident within the positional errors with the H I knot (see Table 1). The formal error ellipse places the infrared source midway between BD +65°1638 and LkHα 234, as shown in Figure 5. In addition the *IRAS* Small Scale Structure Catalogue (1988; SSS) contains an entry (IRAS X2141+658) with a position closer to that of BD +65°1638 (see Table 1 and Fig. 5). HIRES image reconstruction by Eiroa et al. (1998) of the *IRAS*

observations of NGC 7129 indicate the complexity of the region; in these, the brightness distribution peaks nearer to LkHα 234 than to either BD +65°1638 or BD +65°1637.

3.3. *Other* H I *Structures toward NGC 7129*

Among many H I features in this data set only one other structure suggests a physical connection with NGC 7129. A large filamentary structure at $V(\mathrm{lsr}) = -60$ km s^{-1}, reminiscent of the classic shape of a seagull's wings and shown in Figure 8 superposed on a map of the ring, spans the ring structure with its apex coincident with the central H I knot. Despite the large difference in velocity, the morphology alone may suggest a physical association between this filament and the other features discussed above.

The high radial velocity of this structure places it at the edge of the observed bandpass, and thus its true velocity extent is undetermined. Generally, however, similar structures have a velocity width of only about 2 km s^{-1}, and if true in this case the structure would be well represented in our data. The three-dimensional configuration is also not determined: most likely it is filamentary, but we cannot rule out a curved sheet of H I with sufficient optical depth to be observable only where the line of sight is tangent to the surface. As a filament it would have at a distance of 1 kpc a physical width of about 1 pc and a length of about 23 pc. These parameters underline the probable difficulty with such a filament having a velocity of 48 km s^{-1} with respect to the local medium and yet maintaining a small velocity dispersion along its length.

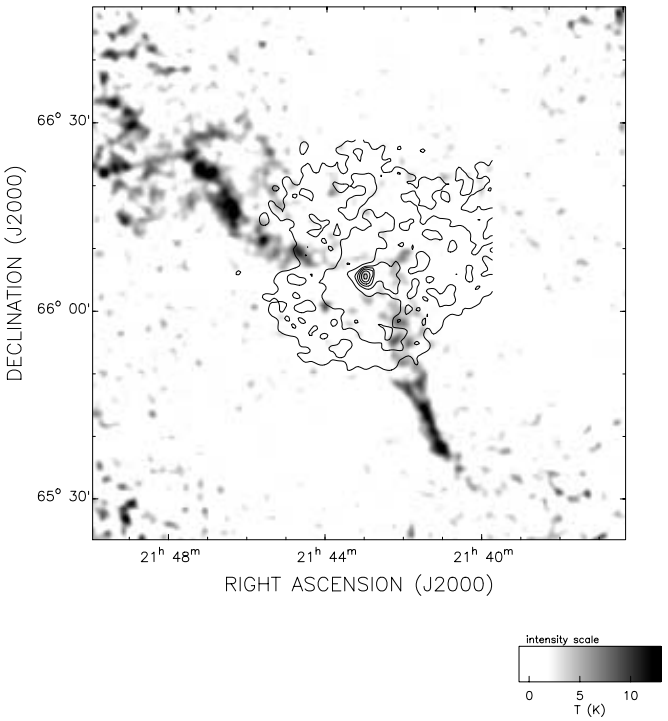

FIG. 8.—Gray-scale image of H I emission averaged over the velocity range −59.7 to −62.6 km s^{-1}, showing the H I "seagull wing" structure (see text). For comparison contours (3–21 K in steps of 3 K over a selected area) are shown of the emission at velocity −12 km s^{-1} (see Fig. 3) to indicate the apparent relation of the H I ring and knot with the extended H I structure. For these data the beamwidth is 1′.5.

4. NATURE OF THE H I RING

We interpret the H I ring as arising in the outer parts of a diffuse interstellar molecular cloud where the molecular hydrogen has been dissociated by incident interstellar ultraviolet radiation, as discussed by Störzer & Hollenbach (1998), Hollenbach & Tielens (1997), Lee et al. (1996), and others. The central parts of this cloud would have given rise to the active star-forming region associated with NGC 7129. Support for this picture on the necessary angular scales is provided by comparisons of the H I emission with optical absorption in the region, mid- and far-infrared images, and large-scale CO observations.

4.1. *Optical and Infrared Images*

Inspection of optical images of the region indicates significant additional interstellar extinction interior to the H I ring when compared with regions outside it. *IRAS* Sky Survey Atlas (ISSA; 1993) images are also indicative of interstellar dust in the same region. We show two of the latter, for 25 and 100 μm, in Figure 9. The infrared emission is dominated by a bright compact source roughly coincident in position with the H I knot, with extended emission particularly to the east and southeast. Progressing through the four *IRAS* wavelength bands from shorter to longer wavelengths this feature appears successively closer to the center of the cloud: it is clearly distinct from the bright central emission at 12 and 25 μm and merges with it at 60 and 100 μm, as seen in Figure 9. As the data at all four wavelengths were convolved to the same angular resolution, a physical cause is suggested; for instance, the observed behavior is consistent with a dust temperature that decreases with depth into the cloud.

4.2. *Associated Molecular Gas*

With angular resolutions of 1′ or less, observations of CO emission show a number of dense molecular clumps in the central 10′ of NGC 7129 (Miskolczi et al. 2001 and references therein). On the larger scale necessary for comparison with our H I data, we used the CO 1–0 CfA survey (Dame, Hartmann, & Thaddeus 2001). Obtained with a beam size of 8′.7, this survey is sensitive to cool diffuse molecular gas and shows several discrete CO clouds in the general vicinity of NGC 7129. The latter coincides with relatively strong CO emission at the southern end of one of these. Superposing the CO and H I emission distributions (Fig. 10) shows that the H I ring is roughly coincident in position with this part of the CO cloud and has comparable width. We expect (see § 4.4) that the H I ring arises as a result of photodissociation of H_2 by interstellar UV radiation in the outer parts of the CO cloud. The apparent positional overlap between the H I and CO images is not exact, but we note that (1) the CO 1–0 survey data were significantly undersampled and (2) since the H I gas is located toward the outside of the CO cloud, projection effects may be important.

After allowing for the beam size, the angular extent of the extended CO cloud is about 61′ × 22′, equivalent to 18 × 6.5 pc at a distance of 1 kpc. We use the empirical relation between cloud mass and CO "luminosity" L_{CO} as defined by Digel et al. (1996) for CO clouds also observed by the CfA telescope to obtain an estimate of the total mass of this cloud. Integrating over the area of the cloud L_{CO} is found to be about 140 K km s^{-1} pc^2, from which we derive a total cloud mass of about 880 $M_\odot$, predominantly in the form of

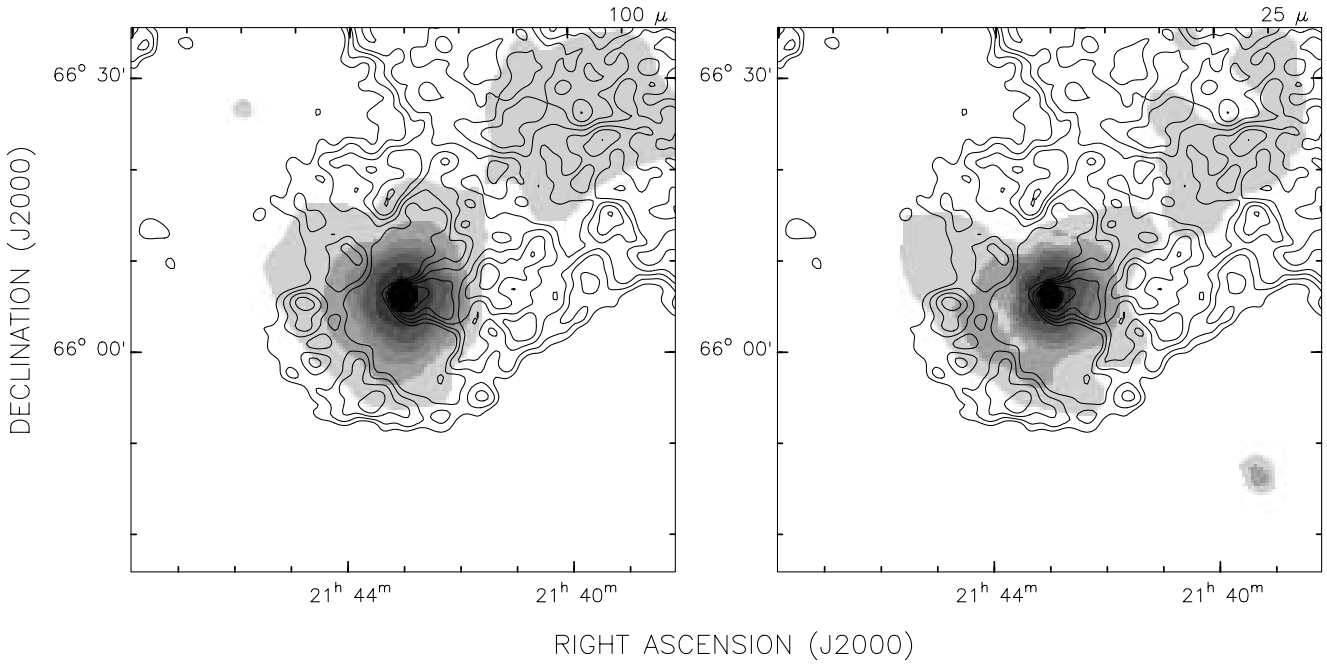

FIG. 9.—Infrared images at 100 μm (*left*) and 25 μm (*right*) obtained from the *IRAS* Sky Survey Atlas (1993). These data, smoothed at all wavelengths to the resolution of the 100 μm data, $\sim 4' \times 5'$, peak strongly at the location of the central stars of NGC 7129. Gray-scale transition levels are 45, 55, 70, 100, 150, 300, and 600 MJy sr^{-1} at 100 μm and 4.7, 5.3, 6.5, 9.0, 15, and 30 MJy sr^{-1} at 25 μm. Contours indicate H I emission as in Fig. 3 and show the location of the H I ring.

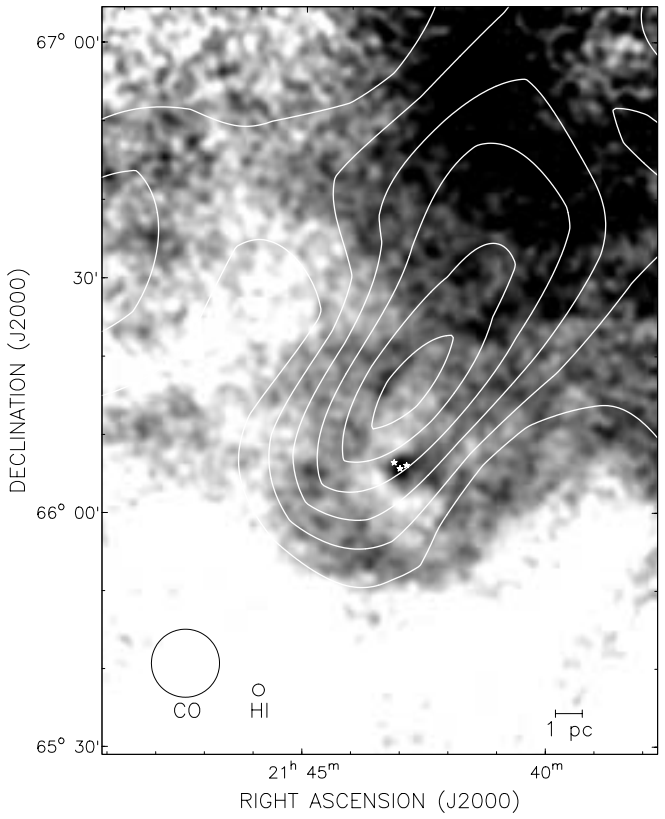

FIG. 10.—Integrated CO 1–0 emission distribution (*contours*) observed with a beam size of 8.′7, taken from the CfA survey (Dame, Hartmann, & Thaddeus 2001) and overlaid on a gray-scale image of NGC 7129 as seen in H I (see also Fig. 3). The CO 1–0 emission was integrated over the velocity range -7.8 to -13.0 km s^{-1}, and the contours run from 0.5 to 3.0 K in steps of 0.5 K. H I emission was integrated over the range -10.2 to -13.1 km s^{-1}. The three stars at the center of NGC 7129 are marked, and the beam sizes to half-power indicated at lower left.

H_2. This falls at the low end of the mass spectrum of the clouds discussed by Digel et al. (1996).

The H I gas has a velocity shift of about -1.5 km s^{-1} with respect to the CO emission, and this needs to be discussed briefly. First, noting the relatively high Galactic latitude of NGC 7129, this velocity difference is consistent in direction and magnitude with the evaporation of H I from the surface of the molecular cloud in response to UV emission from the side facing the Galactic plane. Second, we note that velocity differences of this magnitude between diffuse CO and H I emission are in fact commonplace, when such comparisons have been made. Using the extensive observations of H I surrounding molecular clouds made by Andersson, Wannier, & Morris (1991) and Wannier et al. (1991) and excluding one extreme source (L637), we find that the mean absolute velocity difference between CO and H I is 2.6 ± 3.3 km s^{-1}; hence, the velocity difference between CO and H I of 1.5 km s^{-1} in the present case for NGC 7129 is quite typical.

4.3. *Properties of the* H I *Ring*

While recognizing that the cloud structure in both CO and H I is very inhomogeneous, we can obtain an estimate of the mass of the H I ring by modeling it as a uniform spherical shell. Under this assumption the radial profile of the H I column density was obtained by averaging around annuli centered on the center of the H I ring after subtracting a tilted background from the radial profiles. The result is shown in Figure 11. In this figure material at radii less than 3′ arises in the H I knot and is not included in H I associated with the ring.

This simple model predicts maximum emission along a line of sight tangent to the inner surface of the shell. This occurs at a radius of 12′, which, compared with the outer radius (taken from the profile) of 18′, suggests a shell

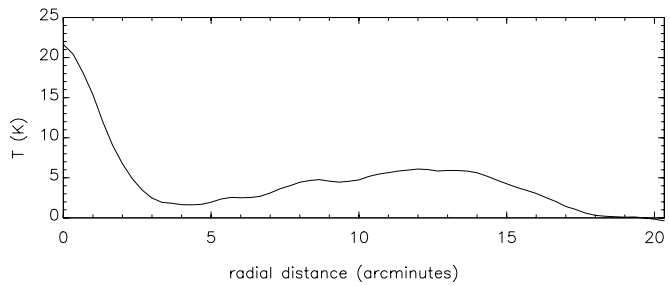

FIG. 11.—Radial profile of the H I ring obtained by averaging within 20″ wide annuli centered on the center of the ring. Data used for averaging were that of Fig. 3. A baseline has been removed for clarity, setting the line temperature to zero beyond the outer radius of the ring.

thickness $\frac{1}{3}$ of the outer radius. At the assumed distance of 1 kpc this corresponds to a shell thickness of 1.8 pc. For this geometry the ratio of maximum to central column density would be about 2.2. To achieve this ratio in the (smoothed) observed radial profile requires a central intensity of 2.5 K, a reasonable value for extrapolation under the emission from the central knot. Over a velocity interval 2.9 km s^{-1} this corresponds to a column density of 1.3×10^{19} cm^{-2}. Combining that with twice the shell thickness gives an average H I density of 1.2 cm^{-3}. There is likely to be an uncertainty of a factor of ± 2 in this value depending on how nearly complete the ring really is (it is potentially confused with H I emission to the northwest) and how much material may have been excluded by using the baseline fits to isolate the ring emission. The average H I density implied is thus within the range of about 0.5–2.5 cm^{-3}.

From these results we can estimate the total H I mass in the shell by integrating the column density over the area of the shell. Using the mean radial profile for this purpose leads to an H I mass of 21 $M_\odot$, with an estimated factor of 2 probable uncertainty. Hence between 1% and 4% of the total H_2 mass of the presumed parent molecular cloud revealed by its CO emission has been photodissociated to form an H I "skin" surrounding the cloud.

4.4. H I *Ring as a PDR*

For comparison with theoretical expectations, the model developed by Lee et al. (1996) addresses the present situation in considerable detail. They consider the development of a surface photodissociation region (PDR) around a low-density molecular cloud immersed in a typical interstellar radiation field. In their model the total hydrogen density $n_H = n(H) + 2n(H_2)$ is 100 cm^{-3} at the surface of the cloud and increases to 400 cm^{-3} at the inner edge of the photodissociated gas. Their steady state solutions (strictly relevant after about 10^8 yr) imply an H I "skin" depth of about 4 pc, in which about half the H I column density arises already from the outer 0.5 pc. By using this model, the H I column density through this skin is about 9×10^{19} cm^{-2}, with the implied average H I density being about 7 cm^{-3}. Given (1) the large uncertainties, (2) the fact that the molecular cloud surrounding NGC 7129 is rather far from the Galactic plane (160 pc) and thus is subjected to a lower level of radiation than considered by Lee et al. (1996), and (3) the rather lower densities in the CO cloud, the observed value, between 0.5 and 2.5 cm^{-3} derived for H I in the outer parts of the NGC 7129 molecular cloud, is in reasonable agreement with the model. Lee et al. (1996) show that H I will be a very minor constituent in such a PDR, the total nucleon density being larger by a factor of about 30. This implies that the latter should be in the range 15–75 cm^{-3} in the NGC 7129 cloud, in rather good agreement with our estimate of about 50 cm^{-3} for the average density derived from the CO 1–0 observations.

The similarity between the models of Lee et al. (1996) and the present data set leads us to conclude that the H I ring is indeed a PDR surrounding a low-density molecular cloud. Given the technical challenge of separating the localized H I in this cloud from the relatively strong H I background, we have nevertheless obtained quite plausible H I density estimates in accord with the model. These data characterize a PDR that is perhaps typical of clouds subjected to the general interstellar radiation field, being considerably weaker than the "H I halos" identified by Wannier et al. (1991) and analyzed by Andersson et al. (1991). The present situation, a 880 $M_\odot$ molecular cloud, is more comparable to those discussed by Andersson, Roger, & Wannier (1992) and Moriarty-Schieven, Andersson, & Wannier (1997), who observed clouds of masses 2000 and 140 $M_\odot$, respectively, also at high Galactic latitudes. However, the distance of the NGC 7129 cloud from the Galactic plane is greater than either of these cases (160 pc vs. 100 and 36 pc, respectively), and hence, we expect a less intense and more asymmetric radiation field in our case, with a resultant lower H I mass, as is observed (21 $M_\odot$, vs. 350 and 48 $M_\odot$, respectively).

5. DISSOCIATION REGION AROUND BD +65°1638

5.1. *BD* +65°1638 *as a Dissociating Star*

The positional coincidences within 10″ of the peak of the H I knot with the star BD +65°1638 and a weak radio continuum source with a flat centimeter-wave spectrum strongly suggest that they are all different physical aspects of the same object. We conclude that BD +65°1638 has given rise to a small H II region surrounded by a more extensive dissociation region of H I. Such "dissociating stars," where the H II region is a very minor part of the system, do not appear to be common. The first to be identified as such, IRAS 23545+6508, was described in detail by Dewdney et al. (1991). Other examples are SVS 3 and BD +30°549 (Rodríguez et al. 1990), LkHα 101 (Dewdney & Roger 1982), and HD 20075 (Rogers, Heyer, & Dewdney 1995).

For an H II region created in a molecular cloud by a young hot star or stars, radiation in the Lyman-Werner bands at wavelengths slightly longer than those of the Lyman continuum will produce a PDR of neutral atomic hydrogen beyond the ionized gas. For relatively cool stars (spectral types B2 through B4, say) the Lyman continuum radiation is weak compared with that in the Lyman-Werner bands, and the resulting mass of gas in the form of neutral hydrogen can be much greater than that in the form of ionized hydrogen by several orders of magnitude. Despite the slow growth of the PDR compared with that of the ionized region (Roger & Dewdney 1992), the dominance of the former can begin at a surprisingly early age.

BD +65°1638 has an apparent visual magnitude of 10.18 (Racine 1968) and $E(B-V) = 0.72$. The absolute visual magnitude derived by Racine (1968) of $M_v = -2.0$ is rather more luminous than would be expected of a B3 zero-age main-sequence (ZAMS) star (Panagia 1973) and suggests a

luminosity class between the ZAMS and class V, probably closer to the latter. Further, the observed continuum flux density of 2.2 ± 0.3 mJy at 1.4 GHz results in an excitation parameter $U = 1.71 \pm 0.2$, appropriate for a star of a somewhat earlier type, about B2.5 (Panagia 1973).

If the H II region associated with BD +65°1638 were created in gas of density 85 cm^{-3} (see § 3.2), we calculate that its angular size would be about 37″. This is in accord with our observation that the associated continuum source is unresolved by the 1′ synthesized beam of the present data set. As we have shown in § 3.2, this result is consistent also with compatible VLA observations (Skinner et al. 1993).

5.2. *Estimating the Age of the Photodissociation Region*

The formation of a PDR around a dissociating star has been modeled by Roger & Dewdney (1992). We have used their computer code to model the specific conditions of BD +65°1638 and its environment. The critical parameters in the computation are the effective stellar temperature and the gas density, which were taken to be 19,000 K (appropriate for a B2.5 star; Panagia 1973) and 85 cm^{-3}, respectively. The results show the PDR increasing in size with time, with the column density in H I across a diameter reaching the observed peak value of 2.6×10^{20} cm^{-2} in an elapsed time of 1500 ± 400 yr. We estimated the uncertainty in this value by varying the density by ± 5 cm^{-3} and the stellar temperature by ± 500 K. Both ranges are likely to be low estimates of the probable errors and both contribute roughly equally to the total uncertainty. Even so, the derived age is *remarkably young*. For confirmation, the code was also run for the specific conditions of IRAS 23545+6508 as given by Dewdney et al. (1991). In the latter case we used a gas density of 300 cm^{-3} and an effective stellar temperature of 18,000 K; these data suggest an even younger age, about 850 yr for IRAS 23545+6508 (Dewdney et al. 1991 quote an age of "less than 10^4 yr").

The computation includes the effects of heating and cooling arising from a variety of mechanisms and calculates the expected temperature in the gas. At age 1500 yr the temperature in the shocked H I close to the ionization front is calculated to be about 2300 K, and falls to about 1400 K in the unshocked H I just outside this region. It then gradually decreases with radius to 330 K at the point where half the H_2 has been dissociated. Although the neutral gas in the central regions is quite warm, more than half the mass of H I lies outside the radius of 50% dissociation, and thus it is difficult to reconcile the temperatures of a few hundred kelvins in those regions with the observed line width without invoking bulk motions.

The surprisingly short ages calculated for dissociating stars, or more specifically for their photodissociation regions, range from 850 to 10^4 yr (including IRAS 23545+6508, the present case, and another example reported by C. R. Purton, W. H. McCutcheon, & M. Normandeau 1999, unpublished). These extremely short time frames suggest either that there is a problem with the modeling or that a very strong selection bias is at work. To investigate the former, various parameters in the computational program (e.g., the rate of re-formation of H_2 on dust grains; see Roger & Dewdney 1992 for details) were changed by a factor of 2 to determine whether the calculated age was particularly sensitive to any of the input parameters. The effects were negligible, with the single exception of the value chosen for turbulent velocity width in the gas. Reducing the latter from 4.0 to 2.0 km s^{-1} increased the age by 17%, not a significant difference in the present context.

We therefore consider the model to be reliable, which in turn implies that a selection bias is at work in dissociating star systems. Over such short timescales, as noted in Roger & Dewdney (1992), the star cannot yet have reached the main sequence and would be somewhat more luminous than a ZAMS star. This would agree with the findings discussed in § 5.1 above. In fact, the stellar temperature and luminosity quoted there place BD +65°1638 exactly on the birthline of a 6 $M_\odot$ star (Palla & Stahler 1993) and support the conclusion from H I modeling that it is indeed very young.

5.3. *Infrared Emission around BD* +65°1638

The physical characteristics of BD +65°1638 and IRAS 23545+6508 (Dewdney et al. 1991) are quite similar, and comparable infrared emission from circumstellar material might therefore be expected for the two cases. The ratios of the 25 and 60 μm fluxes, which we presume to be the more reliable, are $S(21418 + 6552)/S(23545 + 6508) \approx 0.7$. This suggests an integrated infrared flux for IRAS 21418+6552 of $\sim 6 \times 10^{-11}$ W m^{-2}, which corresponds to an infrared luminosity (for a distance of 1 kpc) of $\sim 2 \times 10^3$ $L_\odot$.

Dewdney et al. (1991) were able to use the *IRAS* fluxes to derive a credible bolometric luminosity for IRAS 23545+6508. However, the situation for BD +65°1638 is clearly much more complex, as shown by the HIRES image restoration (Eiroa et al. 1998). The IRAS X2141+658 fluxes, when compared with those of IRAS 23545+6508, suggest a luminosity $\sim 4.4 \times 10^3$ $L_\odot$ for the more distributed far IR emission in the area. This is essentially the same as the value of 4.5×10^3 $L_\odot$ found by Eiroa et al. (1998) for the source they associate with FIRS1 at roughly the same position as IRAS 21418+6552. Under these circumstances it is difficult to derive a bolometric luminosity for BD +65°1638 in isolation from the *IRAS* data. It seems, however, that the *IRAS* fluxes are large enough and the region sufficiently complex so as not to exclude a bolometric luminosity of ~ 2600 $L_\odot$, as is suggested for BD +65°1638 by its absolute visual magnitude (see § 5.1).

5.4. *BD* +65°1638 *Compared with IRAS* 23545+6508

The properties of the two dissociating stars, BD +65°1638 and the prototype IRAS 23545+6508, and their environments are summarized in Table 2. The two systems are remarkably similar. Note that both stars are at a distance of about 1 kpc, a coincidence, that simplifies the comparison of the two systems. The main differences are that (1) the H I velocity dispersion is greater for BD +65°1638 and (2) the radio continuum flux density is larger for BD +65°1638 than for IRAS 23545+6508, suggesting a slightly earlier type for BD +65°1638. The large velocity dispersion found for H I around BD +65°1638, in fact significantly larger than for *any other* dissociating star, is a particularly interesting aspect of this system.

6. ATOMIC AND MOLECULAR GAS AND STAR FORMATION IN NGC 7129

If we accept the interpretations given above of the H I knot and ring, a simple unified model of the NGC 7129

TABLE 2
COMPARISON OF TWO ''DISSOCIATING STARS''

Parameter	BD +65°1638	IRAS 23545+6508[a]
Star:		
Spectral type	B2.5[b]	B3
Distance (kpc)	1.0	1.0
H II:		
Flux density (mJy) [GHz^{-1}]	2.2[1.42]	0.97[4.86]
Diameter (pc)	0.18[b]	0.054
Mass (10^{-3} $M_\odot$)	6.5[c]	0.66
H I:		
Peak column density (10^{20} cm^{-2})	2.6	1.8
Diameter (pc)	1.3 × 0.84	0.93 × 0.44
Density (cm^{-3})	85	133
Mass ($M_\odot$)	1.2	1.42
Velocity dispersion (km s^{-1})	9.0	3.6
Dust:		
IR fluxes (Jy)	15, 79, 688, 1215[d]	48, 136, 764, 1059
IR luminosity ($L_\odot$)	~2000[e]	2703
H_2:[f]		
Geometry (position of H I)	Projected against 1 pc cavity	At peak of 12 pc cloud
Density (cm^{-3})	250	900
Velocity dispersion[g] (km s^{-1})	1.6	2.5

[a] Data taken from Dewdney et al. 1991.
[b] Deduced from radio continuum flux density.
[c] Assuming $n_e = n(\mathrm{H\,I}) = 85$ cm^{-3}.
[d] Taken from *IRAS* PSC, at 12, 25, 60, and 100 μm, respectively.
[e] Scaled to IRAS 23545+6508 via 25 and 60 μm fluxes.
[f] Gas in associated cloud, or in vicinity, as deduced from CO measurements.
[g] Derived from ^{13}CO data.

region is suggested. The entire region lies within an extended molecular cloud, the outer parts of which are photodissociated. Star formation has taken place within this cloud, creating the cavity in the CO distribution first noted by Bechis et al. (1978) and perhaps sweeping some material into denser molecular concentrations (Mitchell & Matthews 1994; Miskolczi et al. 2001), such as that containing LkHα 234, which may have formed subsequently. Two stars, BD +65°1637 and BD +65°1638, appear in projection against the cavity, and the latter is situated inside a photodissociation region.

At first sight it might seem natural to place BD +65°1638 and its attendant H I dissociation region within the CO cavity along with BD +65°1637. We would not expect CO emission to be detected within the H I dissociation region since CO there would also be dissociated by radiation from BD +65°1638, providing a natural explanation for the observed CO cavity.

However, the H I knot extends to the east well beyond the dense CO ridge in which LkHα 234 is situated, itself to the east of BD +65°1638 (cf. Fig. 5 and compare Fig. 1), and does not show any indication of being constrained by or enclosed within the molecular cavity. We therefore suggest that the H I knot is seen in projection against the CO cavity, rather than contained within it. In this case the lack of CO emission can be interpreted as a cavity in the *total* density, as indicated also by submillimeter wavelength continuum observations of dust in the NGC 7129 region (Font, Mitchell, & Sandell 2001). Previous models such as those of Bechis et al. (1978) and Mitchell & Matthews (1994) have suggested that this cavity was created by winds from one or both of the two B stars that appear to lie within it. Bechis et al. (1978) assumed BD +65°1637 to be the younger of the two BD stars largely because it is a Be star, and attribute the wind to BD +65°1638 alone, arguing that its luminosity would be sufficient to create a cavity of the observed size within a reasonable time. However, we have shown in § 5 that BD +65°1638 is instead much the younger of the pair, in fact so young that it cannot be the source of the wind. This therefore requires that the cavity-forming wind originates with BD +65°1637 instead. As support, we note (1) that BD +65°1637 is more luminous than BD +65°1638 (Racine 1968), and hence, following the argument of Bechis et al. (1978), quite capable of producing the cavity and also (2) that BD +65°1637 appears in projection much more centrally located in the CO cavity than does BD +65°1638. Thus the latter, not required as the source of the wind, may well lie outside the cavity altogether, appearing in projection against it.

If BD +65°1638 has indeed formed on the periphery of the cavity and is simply situated along the line of sight through it, the expansion of the cavity could also account for the blueshifted velocity difference of ~1.5–2.0 km s^{-1} between the CO and the peak of the H I knot. In this instance BD +65°1638 would lie on the near side of the CO cavity. Furthermore, Bechis et al. (1978) suggest that the winds have compressed the ambient gas and triggered the recent star formation evident in the CO ridge to the northeast; locating BD +65°1638 on the nearside periphery of the cavity suggests that it too may have a similarly recent origin.

In summary, the limited projected overlap of the H I knot and CO cavity and other considerations suggest they are not spatially coincident but instead that BD +65°1638 and the associated H I knot lie on the front edge of the cavity, along the line of sight.

7. CONCLUSIONS

We have presented and discussed observations of neutral hydrogen emission surrounding NGC 7129, focusing in particular on three distinct features within the data cube. Two of these appear to be associated with the star-forming region on the larger scale—a ring of emission encompassing the entire cloud and a "seagull wing" string of H I emission. Since there is no distance information available in these data the association has to be made primarily on the basis of positional coincidences and correspondence of radial velocities. This seems quite secure in the case of the H I ring but considerably less so for the H I string.

The H I ring appears to be part of the surface of a molecular cloud about 11 pc in extent that contains an active star-forming region (NGC 7129 and environs). Molecular hydrogen on the surface of the cloud has been dissociated by interstellar ultraviolet radiation, producing an H I shell seen in projection as the ring.

The third feature, a bright knot of H I emission with a relatively large velocity width, is coincident within the measurement errors with the young star BD $+65^\circ1638$ and introduces a striking new element into models of the structure of NGC 7129. We have shown that the observations indicate a true physical association of the star with the H I knot and that they are remarkably consistent with BD $+65^\circ1638$ being one of a rare class of "dissociating stars," having an extremely young age of not more than a few thousand years. BD $+65^\circ1638$ itself is found to be a 6 $M_\odot$ star that has just emerged from its cocoon and lies on the birthline calculated by Palla & Stahler (1993).

Dissociation regions around B-type stars are expected to be relatively short lived. Roger & Dewdney (1992) would predict a total lifetime of about 2×10^7 yr for an H I zone around a star like BD $+65^\circ1638$, at which time the ionization front would overtake the dissociation front. However, the extremely young ages derived for the (few) dissociation regions that have been found around B-type stars, together with an apparent lack of more mature such regions, which should be easier to detect, suggest that some other mechanism may further shorten their lifetime. Perhaps the onset of a stellar wind disrupts the ambient gas around the star at an early stage, before the dissociation front can advance to any great distance. If this idea is correct, then the detection of dissociating stars is a means of identifying B-type stars that are very close to the birthline.

Finally, the notion that the circumstellar material is disrupted in the early stages of development of the H I dissociation region may provide an intriguing explanation for the unusually large velocity width of the H I around BD $+65^\circ1638$: it may be that BD $+65^\circ1638$ has advanced to that stage and we are witnessing the first signs of disruption. The relative ages found for the dissociation regions around IRAS 23545+6508 and BD $+65^\circ1638$ and their respective H I velocity widths are consistent with the idea that the latter has reached the disruption stage, while the former has not.

One of us (H. E. M.) is grateful to the Dominion Radio Astrophysical Observatory for warm hospitality and generous assistance during the reduction of the data presented in this paper. C. R. P. is pleased to thank the Joint Astronomy Centre, Hawaii, for the warm welcome and the use of their facilities while working there as a visiting astronomer over the course of several winters. C. R. P. also wishes to thank the Department of Physics at the University of Guelph for their kind hospitality and provision of facilities, which allowed the analysis to be brought to completion during the winter of 2000–2001. Tom Dame (Harvard-Smithsonian CfA) kindly provided the CO 1–0 data used in this paper, and we are pleased to acknowledge insightful comments by an anonymous referee, which resulted in an improved paper. The Digitized Sky Surveys were produced at the Space Telescope Science Institute under US government grant NAG W-2166.

REFERENCES

Andersson, B.-G., Roger, R. S., & Wannier, P. G. 1992, A&A, 260, 355
Andersson, B.-G., Wannier, P. G., & Morris, M. 1991, ApJ, 366, 464
Avila, R., Rodríguez, L. F., & Curiel, S. 2001, Rev. Mexicana Astron. Astrofís., 37, 201
Bechis, K. P., Harvey, P. M., Campbell, M. F., & Hoffmann, W. F. 1978, ApJ, 226, 439
Cabrit, S., Lagage, P.-O., McCaughrean, M., & Olofsson, G. 1997, A&A, 321, 523
Clements, E. D., & Argyle, R. W. 1984, MNRAS, 209, 1
Condon, J. J., Cotton, W. D., Greisen, E. W., Yin, Q. F., Perley, R. A., Taylor, G. B., & Broderick, J. J. 1998, AJ, 115, 1693
Dame, T. P., Hartmann, D., & Thaddeus, P. 2001, ApJ, 547, 792
Dewdney, P. E., & Roger, R. S. 1982, ApJ, 255, 564
Dewdney, P. E., Roger, R. S., Purton, C. R., & McCutcheon, W. H. 1991, ApJ, 370, 243
Digel, S. W., Lyder, D. A., Philbrick, A. J., Puche, D., & Thaddeus, P. 1996, ApJ, 458, 561
Edwards, S., & Snell, R. L. 1983, ApJ, 270, 605
Eiroa, C., Palacios, J., & Casali, M. M. 1998, A&A, 335, 243
English, J., et al. 1998, Publ. Astron. Soc. Australia, 15, 56
Font, A. S., Mitchell, G. F., & Sandell, S. 2001, ApJ, 555, 950
Fuente, A., Martín-Pintado, J., Bachiller, R., Rodríguez-Franco, A., & Palla, F. 2001, A&A, 366, 873
Ghazzali, N., Joncas, G., & Jean, S. 1999, ApJ, 511, 242
Gibson, S., Taylor, A. R., Higgs, L. A., & Dewdney, P. E. 2000, ApJ, 540, 851
Güsten, R., & Marcaide, J. M. 1986, A&A, 164, 342
Hartigan, P., & Lada, C. J. 1985, ApJS, 59, 383
Higgs, L. A. 1999, in ASP Conf. Ser. 168, New Perspectives on the Interstellar Medium, ed. A. R. Taylor, T. L. Landecker, & G. Joncas (San Francisco: ASP), 10
Hollenbach, D. J., & Tielens, A. G. G. M. 1997, ARA&A, 35, 179
IRAS Point Source Catalog. 1988, Joint *IRAS* Science Working Group (NASA RP-1190; Washington: GPO) (PSC)
IRAS Sky Survey Atlas. 1993, ed. S. Wheelock et al. (Pasadena: Caltech) (ISSA)
IRAS Small Scale Structure Catalog. 1988, Version 1.00, ed. G. Helou & D. W. Walker (NASA RP-1190; Washington: GPO) (SSS)
Landecker, T. L., et al. 2000, A&AS, 145, 509
Lee, H.-H., Herbst, E., Pineau des Forêts, G., Roueff, E., & Le Bourlot, J. 1996, A&A, 311, 690
Liseau, R., & Sandell, G. 1983, Rev. Mexicana Astron. Astrofís., 7, 199
Miskolczi, B., Tothill, N. F. H., Mitchell, G. F., & Matthews, H. E. 2001, ApJ, 560, 841
Mitchell, G. F., & Matthews, H. E. 1994, ApJ, 423, L55
Moriarty-Schieven, G. S., Andersson, B.-G., & Wannier, P. G. 1997, ApJ, 475, 642
Palla, F., & Stahler, S. W. 1993, ApJ, 418, 414
Panagia, N. 1973, AJ, 78, 929
Racine, R. 1968, AJ, 73, 233
Ray, T. P., Poetzel, R., Solf, J., & Mundt, R. 1990, ApJ, 357, L45
Rodríguez, L. F., Lizano, S., Canto, J., Escalante, V., & Mirabel, I. F. 1990, ApJ, 365, 261
Roger, R. S., & Dewdney, P. E. 1992, ApJ, 385, 536
Rogers, C., Heyer, M. H., & Dewdney, P. E. 1995, ApJ, 442, 694
Skinner, S. L., Brown, A., & Stewart, R. T. 1993, ApJS, 87, 217
Snell, R. L., & Bally, J. 1986, ApJ, 303, 683
Störzer, H., & Hollenbach, D. 1998, ApJ, 495, 853
Taylor, A. R., et al. 2003, AJ, 125, 3145
Tofani, G., Felli, M., Taylor, G. B., & Hunter, T. R. 1995, A&AS, 112, 299
Wannier, P. G., Andersson, B.-G., Morris, M., & Lichten, S. M. 1991, ApJS, 75, 987
White, G. J., & Gee, G. 1986, A&A, 156, 301